

Cite this: *J. Anal. At. Spectrom.*, 2011, **26**, 1372

www.rsc.org/jaas

PAPER

MC-ICPMS isotope ratio measurements using an ultra-low flow sample introduction system

E. Paredes,^a D. Goitom Asfaha,^a E. Ponzevera,^{†a} C. Brach-Papa,^{‡a} M. Van Bocxstaele,^a J. L. Todoli^b and C. R. Quétel^{*a}

Received 15th December 2010, Accepted 18th February 2011

DOI: 10.1039/c0ja00254b

This study characterises for the first time isotope ratio measurements by multi-collector ICPMS when performed at liquid flow rates as low as 10–15 $\mu\text{L min}^{-1}$. An evolution of the torch integrated sample introduction system (TISIS) was employed, which combined an OpalMist nebulizer and a heated single pass spray chamber, allowing the transport of almost 100% of the solvent. The different factors potentially influencing the isotope ratio measured values and the associated sources of uncertainty (sensitivity and interferences, mass discrimination effects, repeatability of isotope ratio measurement, and rinsing time and memory effects) were investigated systematically under varying experimental conditions. Results showed that the liquid flow rate has a large impact on mass discrimination effects, making the control of this variable critical. From 5 to 30 $\mu\text{L min}^{-1}$, when using the exponential model, the mass discrimination per mass unit changed from -1.6 to -2.1 and from -1.1 to -1.9 , for $^{88}\text{Sr}^+/^{86}\text{Sr}^+$ and $^{208}\text{Pb}^+/^{206}\text{Pb}^+$ ratios respectively. Moreover, extrapolations from these results lead to the conclusion that a syringe pump may be required instead of a free aspiration regime to control the liquid flow rate and eliminate the possibility of undesired variations of isotope ratio results (typically, 0.05‰ error for 1–2% fluctuations at 10 $\mu\text{L min}^{-1}$). The validity of the exponential model also depends on the experimental conditions selected. When working at 15 $\mu\text{L min}^{-1}$ and heating the chamber walls at 60–80 °C, the performance was as good as it could be with a MicroMist/water cooled cinnabar combination operated at 200 $\mu\text{L min}^{-1}$ (thus, the efficiency was 12 times better for the TISIS). Both systems were compared for the measurement of the Sr isotopic signature in honey samples. Since the TISIS allowed for a preconcentration of samples by a factor 5, the combined uncertainty on results could be improved by 1.6 to 4.4. The main drawback was, however, the longer rinsing time required to reach a stable background signal (10–12 minutes rather than 4).

Introduction

The interest in the development of methods for concentration measurements in microsamples has grown in recent years. Several low-flow rate (*i.e.*, around or below 100 $\mu\text{L min}^{-1}$) sample introduction systems have been developed for inductively coupled plasma (ICP) techniques.¹ With the so-called total sample consumption systems there is almost 100% sample transport efficiency, thus giving rise to enhanced sensitivity (and nearly no waste). These systems can be split into two groups. Firstly, those that introduce the aerosol directly into the plasma,

without the use of a spray chamber. This group includes the direct injection nebulizer,² an evolution of it called direct injection high efficiency nebulizer (DIHEN)^{3,4} and the fitting of a conventional micronebulizer to the base of a reduced length torch.^{5,6} Secondly, systems that make use of an evaporation cavity where the solvent is completely vaporized when working at very low liquid flow rates (*i.e.*, around 20 $\mu\text{L min}^{-1}$). Within this group it is possible to differentiate between the so-called torch integrated sample introduction system (TISIS) and several modifications of this design. The TISIS consists of a small cavity placed at the torch base and attached to a shortened plasma injector through a polytetrafluoroethylene adaptor,^{7,8} whereas the modifications are based on the use of a single pass spray chamber instead of the cavity.^{9–12}

For isotope ratio measurements at low liquid flow rates only a few attempts have been made so far. Most of them were based on the use of the DIHEN at liquid flow rates around 60–100 $\mu\text{L min}^{-1}$.^{13–15} Using quadrupole ICP mass spectrometry (MS), when compared with a MicroMist/minicyclonic spray chamber

^aEC—Joint Research Centre—Institute for Reference Materials and Measurements, Retieseweg, 111-2440 Geel, Belgium. E-mail: christophe.quétel@ec.europa.eu; Tel: +32 14 57 1658

^bUniversity of Alicante, Department of Analytical Chemistry, Nutrition and Food Science, Ctra. San Vicente, S/N-03080 Alicante, Spain

[†] Present address: IFREMER, Pointe du diable, 29280 Plouzané, France.

[‡] Present address: IFREMER, rue de l'Île d'Yeu, 44311 Nantes, France.

arrangement working at $85 \mu\text{L min}^{-1}$, the DIHEN was reported to allow an improvement of the isotope ratio repeatability for solutions containing 10 times lower concentrations.¹⁴ For single detector double focusing sector field ICPMS measurements the isotope ratio repeatability was four times worse with a DIHEN than with an ultra-sonic nebuliser at 2 mL min^{-1} .¹³ The alternative to the DIHEN so far is the combination of a micro-nebuliser at $7 \mu\text{L min}^{-1}$ and a single pass spray chamber for transient signals, with repeatability values on uranium isotope ratio measurements not better than 2.3%.¹⁶

The aim of our study was to characterise for the first time isotope ratio measurements by multi-collector (MC) ICPMS under conditions of continuous sample introduction at $10\text{--}15 \mu\text{L min}^{-1}$, using an evolution of the TISIS concept. The purpose was to open new perspectives on small size liquid samples (incl. pre-concentrated samples) without compromising the measurement uncertainty. Preliminary results were presented during the Joint European Stable Isotope Users Meeting in 2008.¹⁷ A systematic assessment of the performance was carried out considering the particularities associated with the use of ultra-low liquid flow rates and the heating of spray chamber walls. The different factors potentially influencing the isotope ratio measured values and the associated uncertainties (sensitivity and interferences, mass discrimination effects, repeatability of isotope ratio measurement, and rinsing time and memory effects) were investigated systematically under varying experimental conditions. The method developed was applied to the determination of the $n(^{87}\text{Sr})/n(^{86}\text{Sr})$ isotope ratio in honey samples from different origins.

Experimental

Instrumentation

All MC-ICPMS measurements were performed using a Nu Plasma 500 (Nu Instruments, Wrexham, UK), equipped with 12 Faraday cups and 3 ion counters. Sensitivity and signal stability were optimised daily by tuning of voltages applied to the extraction and transfer lenses as well as the nebulizer gas flow rate and torch position. These parameters remained unaltered when testing the effect of liquid flow rate and temperature on mass discrimination effects (even over several days successively). Typical operating conditions are reported in Table 1. It must be pointed out that trends shown for the different variables in this manuscript were reproducible over time under these conditions.

The sample introduction system employed was an OpalMist perfluoroalkoxy nebulizer with $10 \mu\text{L min}^{-1}$ natural uptake rate (Glass Expansion, West Melbourne, Australia) and homemade single pass spray chambers which acted as an evaporation cavity according to the principles of the TISIS. Two chambers (SC1 and SC2) with 26 mm i.d. were tested. Differences were in the lengths (100 and 75 mm, respectively) and the slightly different shapes (*i.e.*, radius of curvature) at the exit. The SC1 was jacketed with a copper wire mesh tightly fixed to the walls of the chamber at its entrance and exit (see Fig. 1 for details). This mesh allowed a good contact and the homogeneous heating of the chamber. The heating of the mesh was accomplished by means of a metallic jacket with a thermocouple attached to its surface connected to a temperature controller (Analab, Strasbourg, France). This

system offered several advantages over others based on the use of a heating tape^{12,18} including a more homogeneous contact to the chamber walls; a better stability and a much longer lifetime. The combination of a MicroMist nebulizer with $200 \mu\text{L min}^{-1}$ natural uptake rate (Glass Expansion) and a jacketed minicyclonic spray chamber (Glass Expansion) cooled at 8°C with water (MM-C system) was also used, for comparison purposes.

Acid digestion of honey samples was microwave assisted under high pressure conditions using an UltraClave (Milestone Laboratory systems, Bergamo, Italy). Sample introduction to the TISIS was done *via* two types of syringes: (i) $500 \mu\text{L}$, 3.26 mm i.d. syringe from Kloehn Inc. (Las Vegas, USA), and (ii) 2.5 mL , 7.28 mm i.d. syringe from Ito Corp. (Tokyo, Japan). The working range was 0.01 to $17.65 \mu\text{L min}^{-1}$ for the former and $0.1\text{--}88.0 \mu\text{L min}^{-1}$ for the second one. The liquid flow rate was controlled with a KDS 101 syringe pump (KD Scientific Inc., Holliston, USA).

Samples and materials

Three isotopic certified reference materials were used: a natural-like Sr solution (SRM 987, NIST, Gaithersburg, USA), an 'equal-atom' ^{206}Pb and ^{208}Pb solution (SRM 982, NIST) and a natural-like Zn solution (IRMM-3702, IRMM, Geel, Belgium). These materials were diluted with 3% nitric acid to a final concentration of $500 \mu\text{g L}^{-1}$ for Sr and Pb and $2000 \mu\text{g L}^{-1}$ for Zn. The 3% nitric acid was prepared from 70% ultrapure nitric acid (Ultrex II, J. T. Baker, Phillipsburg, USA) and ultrapure deionized water from a Milli-Q system (Millipore, Bedford, USA). The evaluation of oxides and doubly charged species formation rates were carried out with $250 \mu\text{g L}^{-1}$ Ce and $1000 \mu\text{g L}^{-1}$ Ba solutions, respectively. These solutions were prepared from the corresponding 1000 mg L^{-1} standards (Merck, Darmstadt, Germany) diluted with 3% nitric acid.

The Sr isotopic signature was measured in nine honey samples from different origins (Denmark for 1–3, France for 4–8, and Greece for 9) with both types of sample introduction systems. For 3 of these samples, triplicates were measured with the TISIS and RSDs were compared to MM-C results for another set of 11 samples. After digestion, samples were evaporated to near dryness and taken up back with 8 M HNO_3 for the separation of Sr using a specific crown ether resin (Sr-spec, Eichrom Technologies, Darien, USA). Details about the protocol applied are available elsewhere.¹⁹ Final working solutions of 0.5 or 2.5 mL in 3% HNO_3 were necessary for the TISIS and MM-C measurements, respectively.

Measurement method

Sample introduction and MC-ICPMS acquisitions. Our measurement protocol involved the use of three different syringes (A, B and C) to avoid problems of cross-contamination: syringe A (0.5 mL) to run samples and the SRM 987, syringe B (2.5 mL) for a rinsing step at $40 \mu\text{L min}^{-1}$ for 10–12 minutes with 3% HNO_3 , and syringe C (0.5 mL) to acquire the instrumental background (with 3% HNO_3) and run procedural blank solutions. Syringe A was systematically rinsed off-line successively with milli-Q water (3 times), 3% HNO_3 (2 different solutions, 2 times each) and the next sample itself (3 times with $50 \mu\text{L}$). This

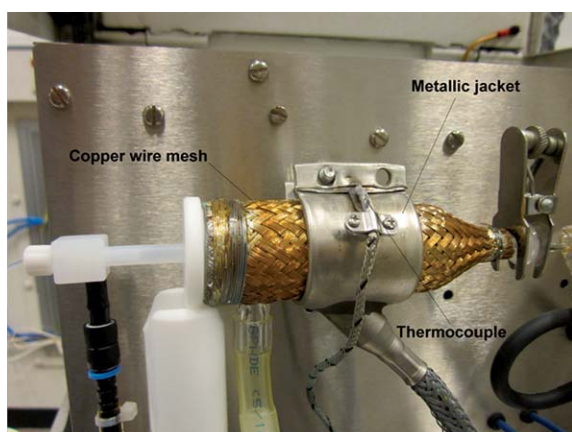
Table 1 Nu Plasma operating conditions with the TISIS

Parameters	Value
<i>Plasma</i>	
RF generator frequency/MHz	27.12
RF Power/W	1300
Coolant gas flow rate/L min ⁻¹	13
Auxiliary gas flow rate/L min ⁻¹	0.89–0.92
Sample gas flow rate/L min ⁻¹	0.80–0.95
<i>Introduction system 1</i>	
Nebulizer	OpalMist
Sample uptake rate/μL min ⁻¹	5–30
Spray chamber	TISIS
Sampler/Skimmer cones	Ni (type A)/Ni (type A-NA)
<i>Introduction system 2</i>	
Nebulizer	MicroMist
Sample uptake rate/μL min ⁻¹	200
Spray chamber	Jacketed minicyclonic
Sampler/skimmer cones	Ni (type A)/Ni (type A-NA)
<i>Mass spectrometer</i>	
Expansion chamber	Brass
Ion energy/V	~4000
Extraction potential/V	2200–2400
Sensitivity ⁸⁸ Sr ⁺ /V per μg g ⁻¹	4 (non-heated)–7 (heated TISIS)
<i>Acquisition</i>	
Number of blocks	1 (Sr); 3 (Pb and Zn)
Replicates per block	30 (Sr); 10 (Pb and Zn)
Integration time/s	10

syringe was then loaded with 200 μL of the same next sample (e.g., consumption of 350 μL of sample in total), and 75 μL of this solution were passed before initiating MC-ICPMS acquisitions. Procedural blanks were measured by series of three at the beginning of each session. The mathematical correction of ⁸⁷Rb⁺ on ⁸⁷Sr⁺ (from the ⁸⁵Rb⁺ signal) was applied whenever the [Sr]/[Rb] ratio was lower than 400 000.¹⁹ Correction for mass discrimination was performed internally by measuring the ⁸⁸Sr⁺/⁸⁶Sr⁺ isotope ratio and using the exponential model (eqn (1)):

$$K = (m_2/m_1)^\epsilon \quad (1)$$

where m_2 and m_1 are the respective atomic masses of the two isotopes considered, ϵ is the mass discrimination per mass unit and K is the 'so-called' K -factor, defined as the ratio of the

**Fig. 1** Picture of the heated spray chamber used in the present work.

measured to the actual isotope ratios. The reference value applied for $n(^{88}\text{Sr})/n(^{86}\text{Sr})$ (ratio of numbers of moles of isotope ⁸⁸Sr and isotope ⁸⁶Sr) was 8.37861 ± 0.00325 ($k = 2$)²⁰ for the SRM 987 whereas for honey samples it was $(1/0.1194) \pm 0$ since this is an internationally accepted consensus value for this ratio²¹ and there was no suspicion of a significant deviation from this value.¹⁹ Recurring measurements of the SRM 987 were performed every 3 samples or blanks to monitor the performance stability of our setup. For 3–4 measurements of this solution taken over 5–8 hours measurement sessions, the reproducibility was always <4% on ⁸⁸Sr⁺ signals and <0.004% on $n(^{87}\text{Sr})/n(^{86}\text{Sr})$ results (corrected for mass discrimination effects).

Uncertainty estimation

All uncertainties were expanded uncertainties ($U_c = ku_c$), with k a coverage factor equal to 2 and u_c combined standard uncertainties obtained by propagating individual uncertainty components according to the ISO/GUM guide.²² In practice, a dedicated software program²³ was used, based on the numerical method of differentiation described by Kragten.²⁴ Additive corrections commonly applied to individual isotope signal intensities measured included those for instrumental background, procedural blank and isobaric interferences. However, since propagating these uncertainties directly with the repeatability of the measurement of isotope signal intensities could lead to an overestimation of u_c , additive corrections were translated into unity multiplicative correction factors on ratios following a method described elsewhere.²⁵

Results and discussion

Sensitivity at ultra-low liquid flow rates

We first investigated the combination of parameters influencing the sensitivity. Our objective was to reach a compromise ensuring both high intensity signals (good counting statistics) and high stability conditions (low noise) for isotope ratio measurement performance. Our criteria of optimisation also included the minimisation, whenever possible, of the formation rates of oxides and doubly charged species. These were measured with cones mounted on a Nu Instruments stainless steel expansion chamber instead of the brass one employed for the rest of experiments (this is possibly affecting the figures of formation rates, but not the trends). For nebulizer gas flow rates (Q_g) ranging from 0.80 to 0.95 L min⁻¹, the signal intensity was found to increase for all the elements tested until a plateau was reached, whereas the formation rate of oxides increased from 0.6 to 8% and the level of doubly charged species decreased from 18 to 11%. Thus, the optimum gas flow rate (0.90–0.92 L min⁻¹) for our experiments resulted from a compromise between sufficient sensitivity and reasonable values of formation rates for oxides (1.5%) and doubly charged species (13.5%).

Effect of the distance nebulizer tip-chamber exit. Two different spray chambers with different lengths were tested at a liquid flow rate of 15 μL min⁻¹. For both chambers it was observed that the further away the nebulizer tip from the chamber exit the greater the sensitivity. For the different configurations tested the optimum Q_g was within the range mentioned above, thus

indicating that the observed trends were not likely due to a modification in the primary aerosol characteristic. The $^{88}\text{Sr}^+$ signal grew up by 40% when increasing the distance between the nebulizer tip and the spray chamber exit from 57 and 64 mm (for SC2). It increased by another 40% when SC1 was used for a distance between the nebulizer tip and the spray chamber exit of 82 mm. These trends are in agreement with those reported for ICPAES¹¹ at higher liquid flow rates (*i.e.*, $28 \mu\text{L min}^{-1}$), where the proposed explanation was the longer the distance between the nebulizer tip and the chamber front walls the lower the risk of losses by impact. The configuration 'SC1 82 mm' was eventually selected for the rest of experiments.

Effect of the sample liquid flow rate. The effect of the sample liquid flow rate (Q_1) at the ordinary temperature inside the torch box (40°C) was tested for three isotopes from elements covering a wide mass range (Fig. 2a). The signal peaked at $15 \mu\text{L min}^{-1}$ for the three isotopes tested, with average sensitivities 4.8, 2.6 and 1.4 times better than at 5, 10 and $30 \mu\text{L min}^{-1}$, respectively. The OpalMist nebulizer is designed to work at $10 \mu\text{L min}^{-1}$ under free aspiration conditions and the lower efficiency found at $30 \mu\text{L min}^{-1}$ may be attributed to an increase in coalescence of droplets.²⁶ At $5 \mu\text{L min}^{-1}$ the signal was very unstable as a consequence of the suction effect of the nebulizer, whereas the repeatability was always better than 3% at liquid flow rates ranging from 10 to $30 \mu\text{L min}^{-1}$. With regard to interferences, the level of oxides increased almost linearly with Q_1 (from $\sim 0.5\%$ at $5 \mu\text{L min}^{-1}$ to $\sim 3\%$ at $30 \mu\text{L min}^{-1}$) whereas the rate of doubly charged species decreased from 18% at $5 \mu\text{L min}^{-1}$ to 10% at $30 \mu\text{L min}^{-1}$. Therefore, with the current configuration, the $15 \mu\text{L min}^{-1}$ liquid flow rate corresponds to the best compromise and is recommended.

Effect of the temperature of spray chamber walls. The heating of the spray chamber walls has the potential to improve significantly the sensitivity for ICPMS^{10,11} and ICPAES¹⁸ systems. As shown in Fig. 2b the sensitivity increased by a factor up to 1.9 upon heating at $65\text{--}85^\circ\text{C}$. This may be attributed to a change in the analyte transport efficiency resulting from the enhanced solvent evaporation when the chamber is heated.¹⁸ This was verified as follows. A 5 mg L^{-1} Sr solution was nebulised for 10 minutes at $15 \mu\text{L min}^{-1}$, assuming that if not transported to the plasma the strontium would deposit on the chamber walls by collision of some droplets (there was no liquid waste visible through the drain). By then rinsing the inside of the TISIS cavity with 3% HNO_3 and measuring the Sr concentration in these rinse solutions, the analyte transport efficiency was estimated to be about 50%, 70% and 80% at 40, 60 and 75°C , respectively. The optimum temperature was, however, slightly fluctuating, and an optimization on a daily basis was necessary. The signal repeatability was better than 3% at temperatures ranging from 40 to 75°C but could degrade up to 6% at higher temperatures. Finally, the heating of the spray chamber had little effect on the oxide formation rate (increase up to 2.5–3% at $60\text{--}80^\circ\text{C}$ and 4.5% at 100°C) and no effect on the formation of doubly charged species.

Comparison against other sample introduction systems. Under these selected conditions ($Q_1 = 15 \mu\text{L min}^{-1}$ and $T = 60\text{--}80^\circ\text{C}$) the OpalMist/TISIS arrangement provided a signal of 3.5 V

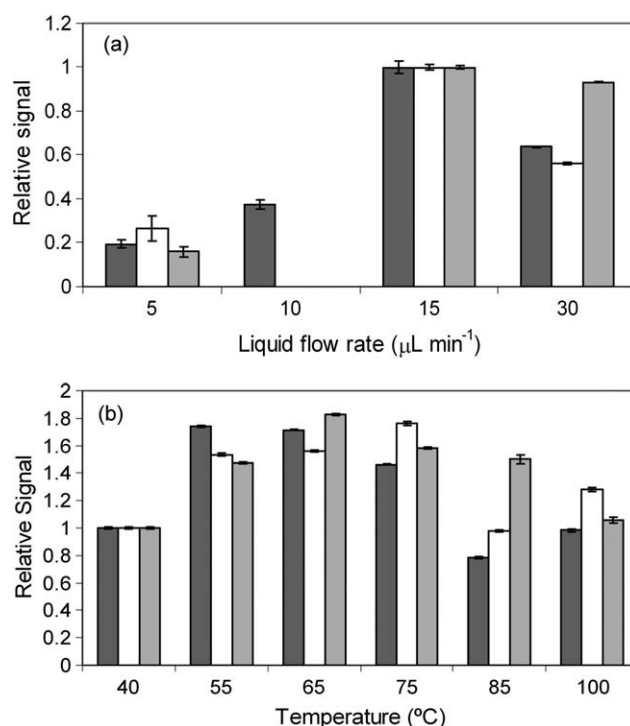


Fig. 2 Variation of the sensitivity for 3 different isotopes with the OpalMist/TISIS arrangement as a function of (a) the liquid flow rate and (b) the temperature (signal normalised to that obtained at $15 \mu\text{L min}^{-1}$ and 40°C). Vertical bars defined as $k \times \frac{s_d}{\sqrt{n}}$ ($k = 2$, $n = 30$). White columns: $^{66}\text{Zn}^+$; dark grey columns: $^{88}\text{Sr}^+$; light grey columns: $^{208}\text{Pb}^+$.

when 7.5 ng of Sr were introduced in 1 minute. To reach the same signal with the MM-C, during the same time interval, 90 ng of Sr needed to be dispensed (thus for nearly the same Sr concentration but at $200 \mu\text{L min}^{-1}$). This is a factor 12 improvement. It also means that smaller size samples can be handled with the TISIS than with the DIHEN since it was reported¹³ that the latter required a liquid flow rate of about $40 \mu\text{L min}^{-1}$ to reach the same sensitivity as the MM-C at $200 \mu\text{L min}^{-1}$. For the MM-C the oxides formation rate was similar to that obtained for the TISIS (2%) whereas a lower percentage of doubly charged species (8.5%) was found.

Mass discrimination at ultra-low liquid flow rates

Main sources of mass discrimination effects during MC-ICPMS measurements, favouring the transmission of heavier ions, are considered to be:²⁷ (i) the nozzle separation effect taking place at the rear part of the sampler, and (ii) space charge effects (also linked to the sample matrix characteristics and the total ion current produced by a sample) after the skimmer and in the ion optics. Other possible sources include changes in RF power, plasma gas and nebulizer gas flow rates, particularly the last one because it influences the dynamic behaviour of the ions in the plasma torch. Furthermore, a mass dependent effect has been recently proposed when using high sensitivity skimmers developed to work under dry plasma conditions.²⁸ Apparently, it is linked to the rate of oxide formation close to the skimmer surface depending on the isotope mass. In the present work, correction

for mass discrimination was internal, *via* the exponential model (eqn (1)).

Influence of liquid flow rate and temperature parameters on mass discrimination effects. Fig. 3a shows the variation of ϵ values at different liquid flow rates (at 40 °C) for Sr and Pb ratios. From 5 to 30 $\mu\text{L min}^{-1}$, ϵ dropped by 0.45 units for $^{88}\text{Sr}^+ / ^{86}\text{Sr}^+$ and by 0.87 units for $^{208}\text{Pb}^+ / ^{206}\text{Pb}^+$. Because no drains were observed at any of the liquid flow rates tested, these large increases in mass discrimination might be attributed to an intensification of space charge effects as the mass of solution delivered to the plasma (liquid flow rate) grew up. Nevertheless, other possible sources linked to a change of plasma characteristics as a consequence of the different loads of solution cannot be ruled out.

With respect to temperature, mass discrimination effects at 15 $\mu\text{L min}^{-1}$ increased from 40 to 55 °C and remained almost constant above. Changes on ϵ were, however, never larger than 0.04, 0.1 and 0.2 units for $^{68}\text{Zn}^+ / ^{66}\text{Zn}^+$, $^{88}\text{Sr}^+ / ^{86}\text{Sr}^+$ and $^{208}\text{Pb}^+ / ^{206}\text{Pb}^+$, respectively. As there was no liquid waste visible, it can be assumed that the solvent load to the plasma remained constant irrespective of the temperature of the chamber. Thus we propose that the evolution of mass discrimination effects with temperature resulted from changes in aerosol characteristics (vapor to liquid ratio) inducing in turn changes to the plasma potential and to the way energy is transferred from the plasma to the analyte. More details about these investigations will be reported in a separate paper.

The influence of the liquid flow rate and the temperature on size and stability of mass discrimination raises the question of possible consequences on uncertainty of isotope ratio measurements for those applications that assume the constancy of mass discrimination effects with time. This is the case of δ -scale measurements, whereby the isotopic signature of a sample is evaluated relatively to the ratio value measured in a reference material (the $\delta=0$ material). Ideally, during the time interval between these two measurements (typically, around 20 minutes or more), biases influencing in a multiplicative way the compared ratios would remain identical. Thus, the calculation of the ratio of these isotope ratios would lead to a mutual cancellation of these biases and hence to an improvement of the overall uncertainty and stability of δ -scale results. However, it was shown that this is not the case for the reliable and reproducible measurement of isotopic variations below 0.05‰ with conventional sample introduction systems.²⁹ We tried to estimate the consequences of fluctuations of the liquid flow rate around 10 $\mu\text{L min}^{-1}$ during ordinary operation of our nebuliser under free aspirating conditions, assuming a linear evolution of ϵ from 5 to 15 $\mu\text{L min}^{-1}$ in Fig. 3a. The range of variations considered (0–5%) is typical of reproducibility values ($n = 3$, aspiration time of 3 min) reported for nebulisers working at $\sim 100 \mu\text{L min}^{-1}$ under free aspiration conditions.³⁰ According to our calculations (Fig. 3b) fluctuations on liquid flow-rate must be lower than 1 and 2% (for Pb and Sr measurements, respectively) to avoid biases bigger than 0.05‰. In order to prevent problems of stability that may characterise the free aspiration mode, we opted for the use of a syringe pump allowing the control of the liquid flow rate with a variability of 0.1% at 10 $\mu\text{L min}^{-1}$. Similar calculations can be made regarding fluctuations on temperature conditions. With the

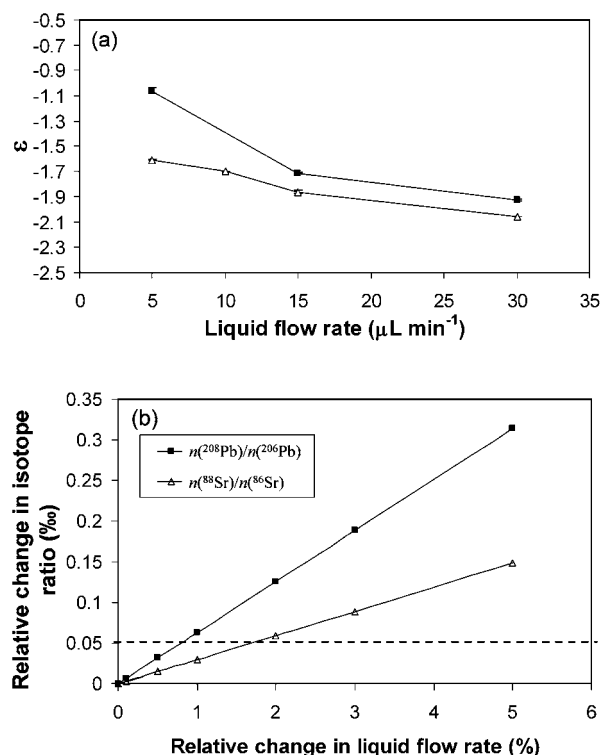


Fig. 3 Effect of the liquid flow rate on the mass discrimination per mass unit value (a) and extrapolations on changes in isotope ratio values that may be induced by 0–5% variations (at 10 $\mu\text{L min}^{-1}$) in liquid flow rate (b). Vertical bars defined as $k \times \frac{s_d}{\sqrt{n}}$ ($k = 2$, $n = 30$). Triangles: $^{88}\text{Sr}^+ / ^{86}\text{Sr}^+$; squares: $^{208}\text{Pb}^+ / ^{206}\text{Pb}^+$.

precision of the temperature controller employed (*i.e.*, ± 1 °C), the bias induced would be smaller than 0.04‰ for Pb isotope ratios (and even smaller for Sr and Zn), thus suggesting that our experimental setup is appropriate for these measurements.

Validity of the exponential model at ultra-low liquid flow rates. What model to use? Several works have challenged the validity of models proposed for the correction for mass discrimination, and linear relationships between ϵ calculated with the exponential model and the average mass of the isotopes involved in the ratios have been reported for some elements.^{31–33} Alternatives proposed to compensate for the deficit of constancy of ϵ in the exponential model include the use of an isotope ratio with similar average mass of the isotopes,³³ or a modification of eqn (1), replacing ϵ with a first-order function of the average mass of the isotopes.³² The slope of this function can vary significantly depending on elements: much flatter for uranium³¹ than for zinc³² in the case of the Nu Plasma. Similar types of differences are observed in this work with the TISIS for Sr and Pb, respectively (Fig. 4). Furthermore, our results show that the validity of the exponential model depended on the liquid flow rate whereas the temperature did not have any significant effect. Slopes obtained at 5, 15 and 30 $\mu\text{L min}^{-1}$ for Sr results were approximately 0.08, 0.02 and 0.01 (Fig. 4a). The last 2 values are similar to the typical slopes obtained with the MM-C working at 200 $\mu\text{L min}^{-1}$. At 5 $\mu\text{L min}^{-1}$ the slope is so steep that it would cause a bias of approximately 0.4‰ on $n(^{87}\text{Sr})/n(^{86}\text{Sr})$ when applying internal

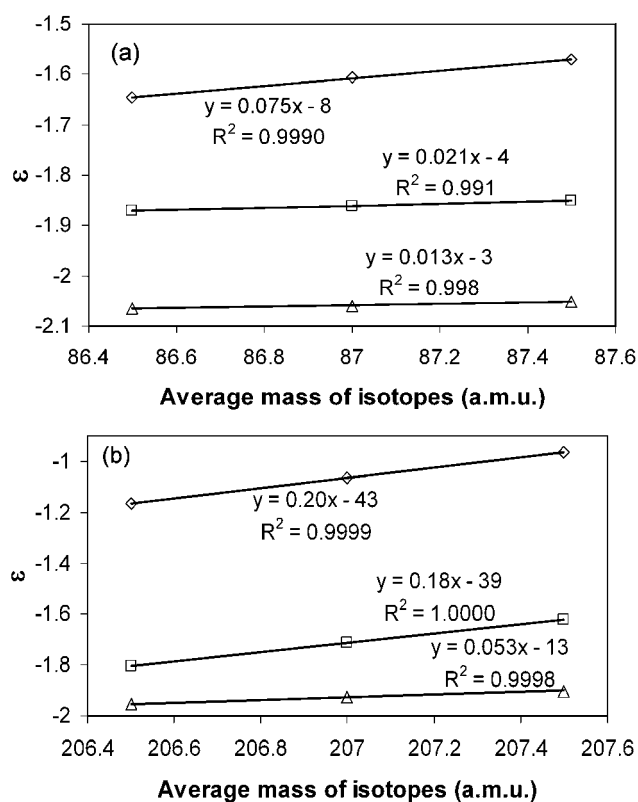


Fig. 4 Effect of the liquid flow rate on the curve ϵ (mass discrimination per mass unit) vs. average mass of isotopes for Sr (a) and Pb (b). Diamonds: 5 $\mu\text{L min}^{-1}$; squares: 15 $\mu\text{L min}^{-1}$; triangles: 30 $\mu\text{L min}^{-1}$.

correction with $^{88}\text{Sr}^{+}/^{86}\text{Sr}^{+}$ isotope ratio using the exponential model. The situation seems to be even more complex in the case of Pb isotope ratios (Fig. 4b), with changes between 15 and 30 $\mu\text{L min}^{-1}$ greater than between 5 and 15 $\mu\text{L min}^{-1}$. These findings underline the possible need for adjustments of the exponential model with this setup depending on the target uncertainty for particular measurements, and the modification proposed for Zn measurements in ref. 32 may be advisable in such cases.

Repeatability of isotope ratio results at ultra-low liquid flow rates

The measurement repeatability for $^{87}\text{Sr}^{+}/^{86}\text{Sr}^{+}$ (non-corrected for mass discrimination) was compared for different liquid flow rates, taken two by two under conditions of identical signal intensities (by adjustment of the Sr concentration in working solutions). About 0.0055% RSEs were obtained at 5 and 15 $\mu\text{L min}^{-1}$ (with ~ 1 V on $^{88}\text{Sr}^{+}$), and 0.0025–0.0035% RSEs were obtained at 15 and 30 $\mu\text{L min}^{-1}$ (with ~ 2 V on $^{88}\text{Sr}^{+}$). Therefore, no significant effect of the liquid flow rate on repeatability of isotope ratios was observed. Similar results were obtained when changing T conditions (RSEs around 0.0035%), except at 100 $^{\circ}\text{C}$ with a degradation. As mentioned above, signal repeatability was degraded at temperatures above 85 $^{\circ}\text{C}$, which could be attributed to the sudden evaporation of droplets as they impact against the walls of the spray chamber.¹¹ This may also introduce some noise in the isotope ratio repeatability. When compared against the MM-C, the OpalMist/TISIS provided repeatability values as good as those obtained with this system despite the use of a liquid

flow rate 13 times lower. RSEs obtained for the $^{87}\text{Sr}^{+}/^{86}\text{Sr}^{+}$ isotope ratio were about 0.0025% for both systems when a solution providing more than 3 V on $^{88}\text{Sr}^{+}$ was run.

On a long term basis (2 months), the reproducibility of $n(^{87}\text{Sr})/n(^{86}\text{Sr})$ results (corrected for mass discrimination) in the SRM 987 solution was 0.005% at 40 $^{\circ}\text{C}$ (RSD, $n = 14$ over 7 different sessions) and 0.010% at the optimum temperature (RSD, $n = 20$ over 8 different sessions).

Rinsing time and correction for memory effects at ultra-low liquid flow rates

It is said in the case of direct injection nebulizers that with total sample consumption systems rinsing times are shortened and memory effects reduced.³⁴ With the TISIS it depends on the dimensions of the chamber used:⁹ the larger the volume of the chamber cavity, the longer the time required to reach the steady state analytical signal and accordingly the longer the rinsing time. More generally, results from the literature relate to concentration measurements and, typically, rinsing times reported correspond to the period required to reach a signal smaller than 1% of that obtained for the measured solution. For isotope ratio measurements with MC-ICPMS, reducing the rinsing time may be even more crucial to reduce the risk of biases between runs. This parameter is not much discussed in the literature and uncertainty components associated to these corrections are even more rarely taken into account (see ref. 19 for an illustration of the way the contribution of the correction for instrumental background and the chemical procedural blank to the expanded uncertainty may be managed). In the present work some unexpected spikes were observed in signals measured for the solution used to acquire the instrumental background even after rinsing at 15 $\mu\text{L min}^{-1}$ for more than 20 minutes. This was likely caused by the re-nebulization of dry analyte particles from the spray chamber walls and the nebulizer tip.¹¹ Application of an ordinary 2- σ outlier rejection routine was not enough to remove these spikes, and the repeatability for background signals remained 20 times worse than for measurements without

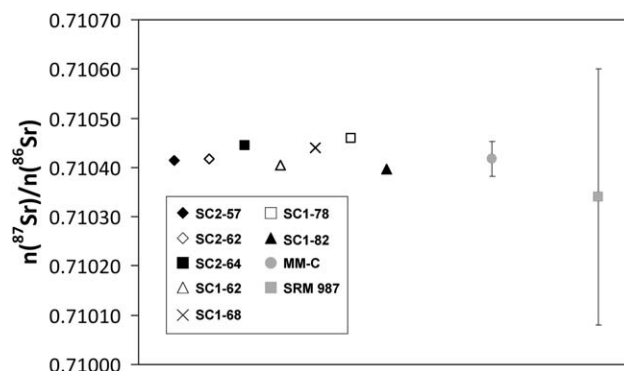


Fig. 5 $n(^{87}\text{Sr})/n(^{86}\text{Sr})$ ratio measurements for a SRM 987 solution (500 $\mu\text{g L}^{-1}$ of Sr in 3% HNO_3) for 7 arrangements of TISIS spray chambers SC1 and SC2 (at 15 $\mu\text{L min}^{-1}$) with different nebulizer tip positions. The number after the dash corresponds to the distance in mm from the nebulizer tip to the exit of the spray chamber. Vertical bars for SRM 987 correspond to the expanded uncertainty ($k = 2$) reported by the provider whereas for MM-C correspond to the typical expanded uncertainty ($k = 2$) obtained with this system.

Table 2 $n(^{87}\text{Sr})/n(^{86}\text{Sr})$ isotope ratios obtained for different honey samples using either the MM-C or the OpalMist/heated TISIS arrangement. Expanded combined uncertainties ($k = 2$) are reported in parentheses and apply to the last two digits

Sample	MM-C	OpalMist/heated TISIS
Honey 1 (Denmark)	0.70888 (44)	0.70915 (15)
Honey 2 (Denmark)	0.70817 (31)	0.70838 (13)
Honey 3 (Denmark)	0.70956 (26)	0.70956 (15)
Honey 4 (France)	0.71501 (72)	0.71566 (17)
Honey 5 (France)	0.71783 (33)	0.71796 (13)
Honey 6 (France)	0.72107 (25)	0.72091 (15)
Honey 7 (France)	0.71916 (50)	0.71920 (15)
Honey 8 (France)	0.71777 (56)	0.71789 (13)
Honey 9 (Greece)	0.71016 (29)	0.71021 (14)

spikes. Spikes were eliminated when the system was rinsed at $40 \mu\text{L min}^{-1}$ for 10–12 minutes. As an additional precaution, acquisition of the background signal was started 5 minutes later after stabilization at $15 \mu\text{L min}^{-1}$. Under these conditions the difference between the maximum and minimum background signals measured for $^{88}\text{Sr}^+$ over 8 hours was less than 3%. Nevertheless, this delay of 15 minutes between samples compares negatively with the MM-C system, for which a stable background signal for the same solution can be reached after rinsing for only 3–4 minutes.

Method validation

The method validation was performed in accordance with the ISO/IEC 17025 guide “General requirements for the competence of testing and calibration laboratories”.³⁵ It was based essentially on a systematic assessment of the factors influencing the results (*cf.* previous sections), a full mathematical description of the measurement process and the establishment of appropriate uncertainty budgets. Equations described in a separate paper for the analysis of mineral waters¹⁹ apply also for this study. The comparison of results obtained with different sample introduction setups corresponds to the case α described in ref. 19. As shown in Fig. 5 for the $n(^{87}\text{Sr})/n(^{86}\text{Sr})$ ratio in the SRM 987, average results ($n = 5$) corresponding to 7 separate TISIS

arrangements were always in agreement with the certified value and with results obtained for the MM-C. The difference relative to the result obtained for the MM-C was ranging from -0.003% to $+0.0055\%$, thus well within the 0.005% ($k = 2$) typical relative uncertainty estimated following the case α approach in ref. 19 for the MM-C result.

Besides, the MM-C and the TISIS were also compared for honey samples, representing a much more complex combination of challenges than simple SRM 987 solutions (results discussed in the next section). In this case the five equations used for the description of the measurement process and the first three contributors to the estimated combined uncertainty were similar to those reported in ref. 19. These were the standard uncertainty associated with the combined corrections for instrumental background, procedural blanks and Rb isobaric interferences (component A), and repeatability values on $^{87}\text{Sr}^+ / ^{86}\text{Sr}^+$ (component B) and $^{88}\text{Sr}^+ / ^{86}\text{Sr}^+$ (component C) measurements. For the fifth equation though, a fourth uncertainty component (here called G) associated to a unity factor multiplied to the Sr ratio was also applied to account for the homogeneity of honey samples. For the purpose of assessing the magnitude of this factor, triplicate measurements were performed on 3 honey samples for the TISIS (average RSD of 0.0144%) and 11 honey samples for the MM-C (average RSD of 0.0153%). The overall average RSD, 0.0151%, includes, however, a contribution from the measurement process that needs to be removed. This contribution was in turn assessed as the RSD of triplicate measurements on the SRM 987 solution (0.003%). Thus, the relative uncertainty component associated to the homogeneity of honey samples could be estimated as the square root of the difference between squares of these end members (0.0148%).

Application to honey samples

This setup was applied to the determination of the Sr isotopic signature in honey samples, typical of the category of environmental/food with heavy matrix characteristics and very low Sr concentration. Digestion methods for honey are complex and prone to contamination (because of manipulations and reagents

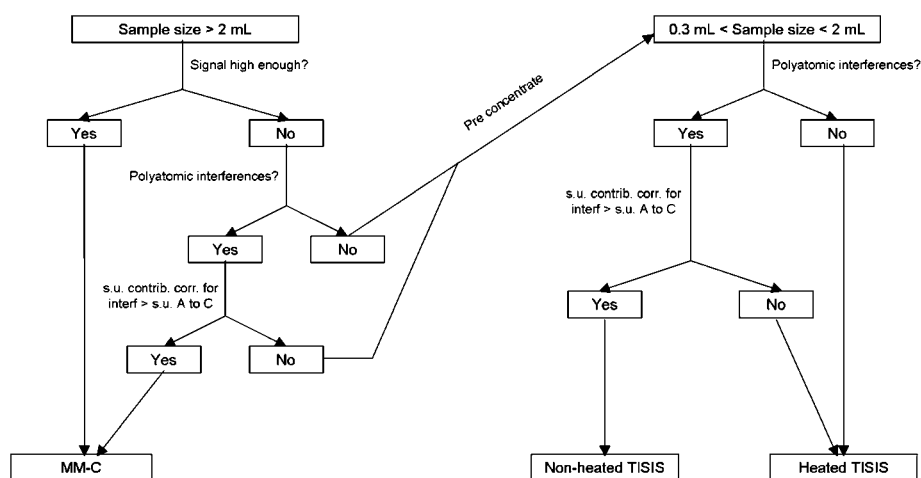


Fig. 6 Decision diagram for the selection of the introduction system most appropriate to the type of liquid sample targeted for as low as possible uncertainties on measurements of isotope ratios with the Nu Plasma.

involved). Besides [Rb]/[Sr] ratios in the original honey samples are rather unfavourable (requiring protocols for intensive Rb separation, with possibly relatively poor rates of recovery for Sr). As a consequence, Sr mass fractions in solutions prepared for introduction with the MM-C can be as low as 15 ng g⁻¹, thus making the measurement under ordinary conditions with a MC-ICPMS of the type we use particularly challenging, if not just impossible (production of inconclusive results due to measurement uncertainty being too high).

Combined uncertainty budgets ($k = 2$) estimated for $n(^{87}\text{Sr})/n(^{86}\text{Sr})$ results in honey samples can be found in Table 2. On average, they were 2.8 times larger for the MM-C results than for the TISIS setup results. This is because of the smaller contributions from uncertainty components A and B (defined in the previous section) in the case of the TISIS setup results owing to the possibility of running more concentrated samples, thus of getting higher signals on $^{87}\text{Sr}^+$ and $^{86}\text{Sr}^+$. Typically, relative contributions to these estimations were for the MM-C and the TISIS setup, respectively, 51% and 24% for A, 32% and 18% for B, 4% and 4% for C and 13% and 54% for G.

Conclusions

Achieving low measurement uncertainty for isotope ratios by MC-ICPMS is not a trivial issue because several factors may contribute. Being able to identify the sample introduction system most appropriate to sample characteristics may be greatly beneficial to the size of this uncertainty. Fig. 6 shows a decision diagram involving considerations based on the size and impact of uncertainty components propagated depending on cases encountered. The MM-C system may be chosen for final samples (*i.e.* after possibly the necessary preliminary steps of digestion and matrix separation) larger than 2 mL and with concentrations of the isotopes of interest guarantying high enough signals (*a priori* ≥ 1 V on $^{88}\text{Sr}^+$ in the case of Sr isotopic measurements). The TISIS may be considered otherwise, except maybe for applications where interferences (such as oxides and doubly charged species) cannot be neglected and they are more abundant for the TISIS. The uncertainty will then depend from factors of degradation (the correction for these interferences) and improvement (components A to C less prominent because of sample preconcentration) that must be estimated before deciding on the most appropriate sample introduction system.

References

- J. L. Todoli and J. M. Mermet, *Spectrochim. Acta, Part B*, 2006, **61**, 239.
- K. E. LaFrenière, G. W. Rice and V. A. Fassel, *Spectrochim. Acta, Part B*, 1985, **40**, 1495.
- J. A. McLean, H. Zhang and A. Montaser, *Anal. Chem.*, 1998, **70**, 1012.
- L. Bendahl, B. Gammelgaard, O. Jøns, O. Farver and S. H. Hansen, *J. Anal. At. Spectrom.*, 2001, **16**, 38.
- J. L. Todoli and J. M. Mermet, *J. Anal. At. Spectrom.*, 2004, **19**, 1347.
- C. S. Westphal and A. Montaser, *Spectrochim. Acta, Part B*, 2006, **61**, 705.
- J. L. Todoli and J. M. Mermet, *J. Anal. At. Spectrom.*, 2002, **17**, 345.
- J. L. Todoli and J. M. Mermet, *J. Anal. At. Spectrom.*, 2002, **17**, 913.
- J. L. Todoli and J. M. Mermet, *J. Anal. At. Spectrom.*, 2003, **18**, 1185.
- W. R. L. Cairns, C. Barbante, G. Capodaglio, P. Cescon, A. Gambaro and A. Eastgate, *J. Anal. At. Spectrom.*, 2004, **19**, 286.
- C. Lagomarsino, M. Grotti, J. L. Todoli and J. M. Mermet, *J. Anal. At. Spectrom.*, 2007, **22**, 523.
- M. Grotti, F. Soggia and J. L. Todoli, *Analyst*, 2008, **133**, 1388.
- J. A. McLean, J. S. Becker, S. F. Bouliga, H.-J. Dietze and A. Montaser, *Int. J. Mass Spectrom.*, 2001, **208**, 193.
- J. S. Becker, H.-J. Dietze, J. A. McLean and A. Montaser, *Anal. Chem.*, 1999, **71**, 3077.
- C. S. Westphal, J. A. McLean, S. J. Hakspiel, W. E. Jackson, D. E. McClain and A. Montaser, *Appl. Spectrosc.*, 2004, **58**, 1044.
- D. Schaumlöffel, P. Giusti, M. V. Zoriy, C. Pickhardt, J. Szpunar, R. Lobinski and J. S. Becker, *J. Anal. At. Spectrom.*, 2005, **20**, 17.
- C. R. Quétel, E. Ponzevera, C. Brach-Papa and J. L. Todoli, *Final Programme and Abstract Book, Joint European Stable Isotope User Meeting*, 2008, p. 40, ISBN: 2-914592-08-6.
- E. Paredes, M. Grotti, J. M. Mermet and J. L. Todoli, *J. Anal. At. Spectrom.*, 2009, **24**, 903.
- C. Brach-Papa, M. Van Bocxstaele, E. Ponzevera and C. R. Quétel, *Spectrochim. Acta, Part B*, 2009, **64**, 229.
- https://www-s.nist.gov/srmors/view_detail.cfm?srm=987.
- R. H. Steiger and E. Jager, *Earth Planet. Sci. Lett.*, 1977, **36**, 359.
- Guide to the Expression of Uncertainty in Measurement*, International Organization for Standardization, Geneva, Switzerland, 1995.
- GUM Workbench, the Software Tool for the Expression of Uncertainty in Measurement*, Metrodata GmbH, Grenzach-Wyhlen, Germany, 2003.
- J. Kragten, *Analyst*, 1994, **119**, 2161.
- C. R. Quétel, T. Prohaska, S. Nelms, J. Diemer and P. D. P. Taylor, in *Plasma Source Mass Spectrometry: the New Millennium, Proceeding of the 7th Durham Conference*, ed. G. Holland and S. Tanner, Royal Society of Chemistry, Cambridge, 2001, p. 257.
- B. L. Sharp, *J. Anal. At. Spectrom.*, 1988, **3**, 939.
- K. G. Heumann, S. M. Gallus, G. Rädlinger and J. Vogl, *J. Anal. At. Spectrom.*, 1998, **13**, 1001.
- K. Newman, P. A. Freedman, J. Williams, N. S. Belshaw and A. N. Halliday, *J. Anal. At. Spectrom.*, 2009, **24**, 742.
- C. R. Quétel, E. Ponzevera, I. Rodushkin, A. Gerdes, R. Williams and J. Woodhead, *J. Anal. At. Spectrom.*, 2009, **24**, 407.
- E. G. Yanes and N. J. Miller-Ihli, *Spectrochim. Acta, Part B*, 2003, **58**, 949.
- C. R. Quétel, J. Vogl, T. Prohaska, S. Nelms, P. D. P. Taylor and P. De Bièvre, *Fresenius' J. Anal. Chem.*, 2000, **368**, 148.
- E. Ponzevera, C. R. Quétel, M. Berglund and P. D. P. Taylor, *J. Am. Soc. Mass Spectrom.*, 2006, **17**, 1412.
- D. Vance and M. Thirlwall, *Chem. Geol.*, 2002, **185**, 227.
- S. E. O'Brien, J. A. McLean, B. W. Acon, B. J. Eshelman, W. F. Bauer and A. Montaser, *Appl. Spectrosc.*, 2002, **56**, 1006.
- ISO/IEC 17025:2005, *General Requirements for the Competence of Testing and Calibration Laboratories*, International Standard Organization, Geneva, 2005.